nature physics

SUPPLEMENTARY INFORMATION

DOI: 10.1038/NPHYS3050

Protecting a spin ensemble against decoherence in the strong-coupling regime of cavity QED

S. Putz[§],[1,2] D. O. Krimer[§],[3] R. Amsüss,[1] A. Valookaran,[1]

T. Nöbauer,[1] J. Schmiedmayer,[1] S. Rotter,[3] and J. Majer[1,2]

[1] *Vienna Center for Quantum Science and Technology, Atominstitut, Vienna University of Technology, Stadionallee 2, 1020 Vienna, Austria*

[2] *Zentrum für Mikro- und Nanostrukturen, Vienna University of Technology, Floragasse 7, 1040 Vienna, Austria*

[3] *Institute for Theoretical Physics, Vienna University of Technology, Wiedner Hauptstrasse 8-10/136, 1040 Vienna, Austria*

(Dated: July 10, 2014)

[§]These authors contributed equally to this work (S.P. experiment, D.O.K. theory)

DOI: 10.1038/NPHYS3050

I. VOLTERRA EQUATION FOR THE CAVITY AMPLITUDE

We start from the Hamiltonian of the main article and derive the Heisenberg operator equations for the cavity and spin operators ($\hbar = 1$), $\dot{a} = i[\mathcal{H}, a] - \kappa a$, $\dot{\sigma}_k^- = i[\mathcal{H}, \sigma_k^-] - \gamma\sigma_k^-$, respectively. Here κ and γ stand for the total cavity and spin losses, respectively. As was shown already in earlier work[1,2] the noise operators can be neglected when considering only expectation values, to which they do not contribute. We also note explicitly that in our calculations the influence of a finite temperature can be disregarded. At the minute temperatures at which the experiment is carried out ($\sim$ 25 mK) we have $k_B T \ll \hbar\omega_s$, resulting in an occupation probability of the ensemble ground state of 99%. Since the number of excited spins remains very small compared to the ensemble size, even with the weak external driving that we use for all the results reported in the main article, we are allowed to apply the commonly used Holstein-Primakoff-approximation, $\langle\sigma_k^z\rangle \approx -1$, when writing down the following set of equations for the operator expectation values in the frame rotating with the probe frequency ω_p. Denoting $A(t) \equiv \langle a(t)\rangle$ and $B_k(t) \equiv \langle\sigma_k^-(t)\rangle$, we end up with the following set of first-order ODEs with respect to the cavity and spin amplitudes

$$\dot{A}(t) = -\left[\kappa + i(\omega_c - \omega_p)\right] A(t) + \sum_k g_k B_k(t) - \eta(t), \tag{1a}$$

$$\dot{B}_k(t) = -\left[\gamma + i(\omega_k - \omega_p)\right] B_k(t) - g_k A(t). \tag{1b}$$

Note, that the size of our spin ensemble is very large (typically $N \sim 10^{12}$) and individual spins are distributed around a certain mean frequency ω_s. We can thus go to the continuum limit by introducing the continuous spectral density as $\rho(\omega) = \sum_k g_k^2 \delta(\omega - \omega_k)/\Omega^2$ (see, e.g. 1), where Ω is the collective coupling strength of the spin ensemble to the cavity and $\int d\omega\rho(\omega) = 1$. In what follows we will replace any discrete function $F(\omega_k)$ by its continuous counterpart, $F(\omega)$: $F(\omega_k) \to \Omega^2 \int d\omega\rho(\omega)F(\omega)$. By integrating Eq. (1b) in time, each individual spin amplitude, $B_k(t)$, can formally be expressed in terms of the cavity amplitude, $A(t)$. By plugging the resulting equation into Eq. (1a) and assuming that initially all spins are in the ground state, $B_k(t = 0) = 0$, we arrive at the following integro-differential Volterra equation for the cavity amplitude ($\omega_c = \omega_s$)

$$\dot{A}(t) = -\kappa A(t) - \Omega^2 \int d\omega\rho(\omega) \int_0^t d\tau e^{-i(\omega-\omega_c-i\gamma)(t-\tau)} A(\tau) - \eta(t), \tag{2}$$

Note that in the ω_p-rotating frame the rapid oscillations presented in the original Hamiltonian (1) are absent, so that the time variation of $\eta(t)$ in Eq. (2) is much slower as compared to $1/\omega_p$.

For a proper description of the resulting dynamics, it is essential to capture the form of the spectral density $\rho(\omega)$ realized in the experiment as accurately as possible. Following 3, we take the q-Gaussian function for that purpose

$$\rho(\omega) = C \cdot \left[1 - (1-q)\frac{(\omega-\omega_s)^2}{\Delta^2}\right]^{\frac{1}{1-q}}, \tag{3}$$

characterized by the dimensionless shape parameter $1 < q < 3$ which yields the form of a Lorentzian and Gaussian distribution, for $q = 2$ and for $q \to 1$, respectively. Here C is a normalization constant which is easily obtained numerically; the full-width at half-maximum (FWHM) of $\rho(\omega)$ is given by $\gamma_q = 2\Delta\sqrt{\frac{2^q-2}{2q-2}}$.

In a next step we formally integrate Eq. (2) in time to get rid of the time derivative of $A(t)$. The resulting double integral with respect to time on the right-hand side is simplified further by partial integration, so that we obtain again a single integral with respect to time. Assuming that the cavity is initially empty, $A(t=0) = 0$, we finally end up with the following equation for the cavity amplitude

$$A(t) = \int_0^t d\tau \mathcal{K}(t-\tau)A(\tau) + \mathcal{F}(t), \tag{4}$$

which contains the kernel function $\mathcal{K}(t-\tau)$,

$$\mathcal{K}(t-\tau) = \Omega^2 \int d\omega \, \frac{\rho(\omega)\left[e^{-i(\omega-\omega_c-i(\gamma-\kappa))(t-\tau)} - 1\right]}{i(\omega-\omega_c-i(\gamma-\kappa))} \cdot e^{-\kappa(t-\tau)}, \tag{5}$$

and the function $\mathcal{F}(t)$,

$$\mathcal{F}(t) = -\int_0^t d\tau \, \eta(\tau) \cdot e^{-\kappa(t-\tau)}. \tag{6}$$

Despite its seemingly simple form, Eq. (4) is not trivial to solve in practice, even numerically. The reasons are twofold: First, the result of the integration for $A(t)$ at time t depends on the amplitude $A(\tau)$ calculated at all earlier times, $\tau < t$ (memory effect). Second, the kernel function $\mathcal{K}(t-\tau)$ contains the integration with respect to frequency, which is costly in terms

DOI: 10.1038/NPHYS3050

of computational time. (Note that such an integration has to be performed for each t and $\tau < t$.) The smallest possible time scale in our problem is given by $T = 2\pi/\omega_p \sim 0.4\,\mathrm{ns}$. To achieve a very good accuracy of the calculations for the results presented in Figs. 2,4 from the main article, we solve the equation on a mesh with uniform spacing, choosing a time step $dt \sim 0.05\,\mathrm{ns}$ (see e.g. 4 for more details about the method). The direct discretization of $\mathcal{K}(t-\tau)$ on the time interval of the order of μs (typical time of measurements) leads to a high-dimensional matrix (of a size typically exceeding $10^4 \times 10^4$), which, together with the integration with respect to frequency, makes the problem computationally intractable by way of a direct numerical solution. To overcome this problem and to speed up the calculations drastically, we divide the whole time integration into many successive subintervals, $T_n \leq t \leq T_{n+1}$, with $n = 1, 2, ...$ Such a time division might, in principle, be implemented arbitrarily but we choose it to be adapted to our experimental realization. Specifically, the driving amplitude is unchanged within each subinterval, so that in our case it is given by

$$\eta_n = \begin{cases} \eta & n = 1, 3, 5, ... \\ -\eta & n = 2, 4, 6, ... \end{cases}. \tag{7}$$

In this way the result of integration at the n-th time interval, $A^{(n)}(T_{n+1})$, enters as an initial condition for the integration during the $(n+1)$-th time interval, $A^{(n+1)}(T_{n+1})$. Finally, we end up with the following recurrence relation (time runs within $T_n \leq t \leq T_{n+1}$ for $n = 1, 2, 3, ...$)

$$A^{(n)}(t) = \int_{T_n}^{t} d\tau \mathcal{K}(t-\tau) A^{(n)}(\tau) + \mathcal{F}^{(n)}(t), \tag{8}$$

where the kernel function $\mathcal{K}(t-\tau)$ is defined by Eq. (5) and

$$\mathcal{F}^{(n)}(t) = A^{(n-1)}(T_n) e^{-\kappa(t-T_n)} + \Omega^2 e^{-\kappa(t-T_n)} \int d\omega \frac{\rho(\omega)\left[e^{-i(\omega-\omega_c-i(\gamma-\kappa))(t-T_n)} - 1\right]}{i(\omega-\omega_c-i(\gamma-\kappa))} \cdot \mathcal{I}_n(\omega) - \frac{\eta_n}{\kappa} \cdot \left[1 - e^{-\kappa(t-T_n)}\right] \tag{9}$$

Remarkably, the memory about previous events enters both through the amplitude $A^{(n-1)}(T_n)$ and through the function

$$\mathcal{I}_n(\omega) = e^{-i(\omega-\omega_p-i\gamma)(T_n-T_{n-1})} \mathcal{I}_{n-1}(\omega) + \int_{T_{n-1}}^{T_n} d\tau e^{-i(\omega-\omega_p-i\gamma)(T_n-\tau)} A^{(n-1)}(\tau). \tag{10}$$

In accordance with the above initial conditions ($t = T_1 = 0$), $A(T_1) = 0$ and $\mathcal{I}_1(\omega) = 0$.

The above technique allows us to solve Eq. (4) accurately while being very efficient in terms of computational time. We have tested the accuracy of our numerical results by varying the discretization both in time and frequency in a wide range obtaining excellent agreement with the experimental results shown in Figs. 2,4 of the main paper and thereby confirming the accuracy of our method.

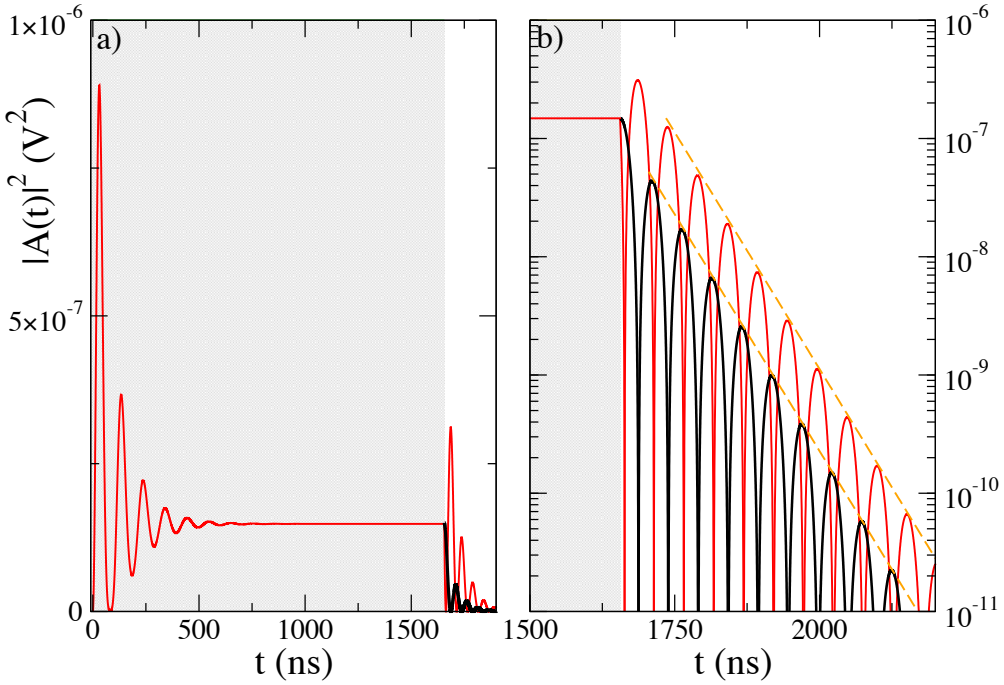

FIG. 1: a) Red curve: calculated cavity probability amplitude $|A(t)|^2$ versus time t under the action of an incident long multi-photon pulse of duration 1.65 μs with the carrier frequency matching the resonance condition, $\omega_p = \omega_c = 2\pi \cdot 2.6915\,\mathrm{GHz}$, and the coupling strength $2\Omega = 17.2$ MHz (analogous to Fig. 2b from the main article). Gray (white) area indicates a time interval during which a pumping signal is on (off). Black curve: Decay from the initial state $|1, G\rangle$, for which a single photon with frequency ω_c is in the cavity and all spins are in the ground state. For the sake of visualisation, the initial probability is rescaled such as to coincide with the steady state value of the multi-photon signal. b) Same figure as a) with a zoom on the decaying part and with the ordinate plotted on a logarithmic scale. The asymptotic decay is well described, for both the red and the black curve, by the exponential function, $C\,e^{-\Gamma t}$, with $\Gamma/2\pi = 3.0\,\mathrm{MHz}$ taken from Fig. 3 of the main article (see orange dashed curves). This agreement illustrates the applicability of the cavity-protection effect also for single-photon processes.

DOI: 10.1038/NPHYS3050

II. CAVITY PROTECTION EFFECT ON THE SINGLE PHOTON LEVEL

In the experiment presented in the main article the number of microwave photons in the cavity is typically of the order of 10^6. Here we demonstrate that our main findings on the cavity protection effect also remain valid when only a single photon is populating the cavity. For this purpose we start from the Heisenberg equations for the cavity and spin operators, $a(t)$ and $\sigma_k^-(t)$, which have the same form as those described in Sec. I. We now assume that the cavity is fed with a single photon and all spins are in the ground state, $|1,G\rangle = a^\dagger(t=0)|0\rangle$, where $|0\rangle$ stands for the vacuum state. We then let these operator equations act on the bra- and ket-vectors $\langle 0|$ and $a^\dagger(t=0)|0\rangle$, respectively, and derive the corresponding equations for the expectation values. These equations perfectly coincide with Eqs. (1a,1b) from Sec. I where, however, the amplitudes $A(t), B(t)$ are now given as $A(t) \equiv \langle 0|a(t)a^\dagger(t=0)|0\rangle$ and $B_k(t) \equiv \langle 0|\sigma_k^-(t)a^\dagger(t=0)|0\rangle$. Note that the variable $A(t)$ stands here for the probability amplitude for a photon to be in the cavity at time t, if it was there initially, $A(t=0) \equiv \langle 0|a(t=0)a^\dagger(t=0)|0\rangle = \langle 1,G|1,G\rangle = 1$.

We thus find for the single-photon regime the same Volterra equation for the cavity amplitude, $A(t)$, as we did before for the multi-photon decay process from the steady-state as considered in the main article (see Fig. 3 there). The only difference lies in the initial condition, which, in the single-photon case, takes on the simple form $A(t=0) = 1$. However, the asymptotic decay rate Γ is independent of the initial conditions and the cavity protection effect remains unaffected. To demonstrate this explicitly also numerically, we compare in Fig. 1 the multi-photon dynamics from the main text with the single-photon case considered here. At first sight, the decay dynamics look very different in these two cases, see Fig. 1a), even when the probability $|A(t)|^2$ is rescaled for both cases to coincide at $t = 0$. When plotting the decay logarithmically, see Fig. 1b), it becomes clear, however, that the asympotitic decay constants which are relevant for the cavity protection effect are, indeed, exactly the same. To conclude, the key insight on the reduction of the decay rate for increasing collective coupling strength Ω (as following from Fig. 3 of the main article), remains valid also on the single-photon level.

[1] Diniz, I. *et al.* Strongly coupling a cavity to inhomogeneous ensembles of emitters: Potential for long-lived solid-state quantum memories. *Phys. Rev. A* **84**, 063810 (2011). 2

[2] Kurucz, Z., Wesenberg, J. H. & Mølmer, K. Spectroscopic properties of inhomogeneously broadened spin ensembles in a cavity. *Phys. Rev. A* **83**, 053852 (2011). 2

[3] Sandner, K. *et al.* Strong magnetic coupling of an inhomogeneous nitrogen-vacancy ensemble to a cavity. *Phys. Rev. A* **85**, 053806 (2012). 3

[4] Press, W. H., Teukolsky, S. A., Vetterling, W. T. & Flannery, B. P. Numerical recipes: The art of scientific computing. *Cambridge University Press, New York* (2007). 4